Multisatellite observations of the magnetosphere response to changes in the solar wind and interplanetary magnetic field

Galina Korotova[1,2], David Sibeck[3], Scott Thaller[4], John Wygant[4], Harlan Spence[5], Craig Kletzing[6], Vassilis Angelopoulos[7], and Robert Redmon[8]

[1]IPST, University of Maryland, College Park, MD, USA
[2]IZMIRAN, Russian Academy of Sciences, Moscow, Troitsk, Russia
[3]Code 674, NASA/GSFC, Greenbelt, MD, USA
[4]College of Science and Engineering, University of Minnesota, Minneapolis, MN, USA
[5]EOS, University of New Hampshire, Durham, NH, USA
[6]Department of Physics and Astronomy, Iowa University, Iowa City, IA, USA
[7]Department of Earth, Planetary and Space sciences, UCLA, Los Angeles, CA, USA
[8]Solar and Terrestrial Physics division, NGDC/NOAA, Boulder, CO, USA

Abstract

We employ multipoint observations of the Van Allen Probes, THEMIS, GOES and Cluster to present case and statistical studies of the electromagnetic field, plasma and particle response to interplanetary (IP) shocks observed by Wind. On February 27, 2014 the initial encounter of an IP shock with the magnetopause occurred on the postnoon magnetosphere, consistent with the observed alignment of the shock with the spiral IMF. The dayside equatorial magnetosphere exhibited a dusk-dawn oscillatory electrical field with a period of ~ 330 s and peak to peak amplitudes of ~ 15 mV/m for a period of 30 min. The intensity of electrons in the energy range from 31.5 to 342 KeV responded with periods corresponding to the shock induced ULF electric field waves. We then perform a statistical study of Ey variations of the electric field and associated plasma drift flow velocities for 60 magnetospheric events during the passage of interplanetary shocks. The Ey perturbations are negative (dusk-to-dawn) in the dayside magnetosphere (followed by positive or oscillatory perturbations) and dominately positive (dawn-to-dusk direction) in the nightside magnetosphere, particularly near the Sun-Earth line within an L-shell range from 2.5 to 5. The typical observed amplitudes range from 0.2 to 6 mV/m but can reach 12 mV during strong magnetic storms. We show that electric field perturbations increase with solar wind pressure and that the changes are especially marked in the dayside magnetosphere. The direction of the Vx component of plasma flow is in agreement with the direction of the Ey component and is antisunward at all local times except the nightside magnetosphere, where it is sunward near the Sun-Earth line. The flow velocities Vx range from 0. 2 to 40 km/s and are a factor of 5 to 10 times stronger near noon as they correspond to greater variations of the electric field in this region. We demonstrate that the shock-induced electric field signatures can be classified into four different groups according to the initial Ey electric field response and these signatures are local time dependent. Negative and bipolar pulses predominate on the dayside with positive pulses occur on the nightside. The ULF electric field pulsations of Pc and Pi types produced by IP shocks are observed at all local times and in the range of periods from several tens of seconds to several minutes. We believe that that most electric field pulsations of the Pc5 type in the dayside magnetosphere at L < 6 are produced by field line resonances. We show that the direction of the shock normal determines the direction of the propagation of the shock-induced magnetic and plasma disturbances. The observed directions of velocity Vy predominately agree with those expected for the given spiral or orthospiral shock normal orientation.

Keywords: Interplanetary shocks, solar wind – magnetosphere interactions, energetic particles, trapped.

1 Introduction

Sudden increases in the solar wind dynamic pressure accompanying interplanetary (IP) shocks cause earthward motion of the bow shock and the magnetopause and launch fast and intermediate mode waves into the magnetosphere (Tamao, 1964). The fast mode waves propagate both radially inward and azimuthally around the Earth (Araki et al., 1997) whereas the intermediate mode waves propagate along magnetic field lines to produce transient perturbations in the high-latitude dayside ionosphere (Southwood and Kivelson, 1990; Glaßmeier and Heppner, 1992). Using multipoint observations) estimated the propagation speeds to be about 600 km/s in the radial direction from geostationary orbit to the ground and about 910 km/s in the azimuthal direction in the equatorial plane. Nopper et al. (1982) estimated an impulse disturbance speed of about 1500 km/s at geostationary orbit. Schmidt and Pedersen (1988) derived a propagation velocity for the radially inward travelling compressive wave of 950 km/s and for the azimuthal wave in the outer magnetosphere of 1100 km/s. Samsonov et al. (2007) used a magnetohydrodynamic code to simulate the interaction of a moderately strong interplanetary shock propagating along the Sun-Earth line and obtained the average speed of the primary and reflected fast shocks in the magnetosphere to be about 700 km/s, in agreement with their assumptions concerning the mean Alfvén velocity in the outer dayside magnetosphere (1000 km/s) and in the plasmasphere (500 km/s).

The IP shock orientation plays an important role in determining the associated geophysical effects (e.g., Oliveira and Raeder, 2015) showed that system evolution times are much longer for shocks with normals oblique to the Sun–Earth line. The pressure pulse model of Sibeck (1990) predicts dawnward moving transient events near local noon when shock normals point perpendicular to the nominal spiral interplanetary magnetic field (IMF) direction, but duskward moving events occur near local noon for events when shock normals point perpendicular to the orthospiral IMF orientation. The direction of the plasma flow within the magnetosphere is expected to be consistent with the orientation of the shock. That is to say dawnward flow for spiral IMF shocks and duskward flow for orthospiral IMF shocks. Here orthospiral refers to IMF longitudes ($0^o < \Lambda < 90^o$ and $180^o < \Lambda < 270^o$), spiral refers to IMF longitudes ($90^o < \Lambda < 180^o$ and $270^o < \Lambda < 360^o$), where longitude $\Lambda=0^o$ points sunward, and $\Lambda=90^o$ duskward.

The magnetic and electric fields are key parameters for understanding of the response of the Earth's space environment to IP shocks. The propagation and evolution of electric fields in the magnetosphere-ionosphere system in response to IP shocks have been studied for several decades but signatures of the shock related electric field perturbations are still not fully understood. Knott et al. (1985) reported that the electric field observed by the GEOS-2 satellite showed a transient signature of about 7 mV/m in the dayside magnetosphere associated with the onset of a Sudden Commencement (SC). These signatures were followed by Pc4-5 oscillations. Schmidt and Pedersen (1988) performed a statistical investigation of the GEOS2 electric field signatures associated with SC that showed a clear tailward flow pattern near local noon. Close to the flanks or in the nightside of the magnetosphere the corresponding flows also exhibited a radially inward component. Shinbory et al (2004) investigated the detailed signatures of the Akebono electric and magnetic fields associated with SCs inside the plasmasphere ($L < 5$). The initial excursion of the electric field associated with SCs was almost directed westward at all local times. The amplitude did not show a clear dependence on magnetic local time and the intensity of the Ey field gradually increased by 0.5-2.0 mV/m about 1-2 minutes after the onset of the initial electric field impulse. The propagation velocity of SCs disturbances derived from the amplitude ratio of the electric field to magnetic field was about 360 km/s in the equatorial plasmasphere. Kim et al. (2009) used an MHD simulation to examine the electric field and suggested that the SC associated electric field seen by Shinbory et al. (2004) was the convection electric field. Takahashi et al. (2017) investigated the spatial and temporal evolution of large-scale electric fields in the magnetosphere and ionosphere associated with SCs using multipoint equatorial magnetospheric and ionospheric satellites together with ground radars and showed that the propagation characteristics of electric fields in the equatorial plane depend on magnetic local time. They showed that the initial variation of the electric field (negative Ey) lasted about one minute and was directed westward throughout the inner magnetosphere. Positive Ey became dominant 2 min after SCs propagated to pre-midnight or post-midnight region with near costant amplitude.

Observations and MHD simulations (e.g., Li et al., 1993; Zong et al., 2009; Halford et al., 2014; Schiller et al., 2016) show that the electric fields generated by sudden compressions can resonantly interact with trapped charged particle populations within the Earth magnetosphere, energizing and injecting them deep into the magnetosphere. During the well-known shock event in March 1991, the CRESS satellite observed injected electrons energized to extremely high energies, up to 5 MeV (Blake et al., 1992). Wygant et al. (1994) showed that the shock related electric and magnetic field perturbations observed by the CRRES satellite in the nightside inner magnetosphere exhibited a bipolar waveform with amplitude of about 80 mV/m and 140 nT, respectively, and energized the energetic electrons to energies up to 15 MeV. Foster et al. (2015) found that a shock with an azimuthal electric field impulse of 10 mV/m observed by the Van Allen Probes was responsible for accelerating 1.5-4.5 MeV electrons by 400 KeV in the radial region of L= 3.5-4.

This paper focuses on two major issues. We will inspect multispacecraft electric and magnetic field and particles and plasma observations to study their response to an IP shock on February 27, 2014. We will time the occurrence of magnetic field disturbances associated with the shock in space and the magnetosphere and will show that it propagated dawnward consistent with expectations based on the shock orientation. Then we will perform a statistical study of the

Van Allen Probes electric field disturbances in the magnetosphere and associated plasma drift Vx and Vy velocities in response to IP shocks. We will show that there are four categories of electric field perturbations that occur in response to shock-induced compressions and that these signatures have a clear dependence on magnetic local time. We will show that the direction of the shock normal has an important effect on the propagation of the shock induced magnetic and plasma disturbances and that our statistical results are consistent with MHD simulation prediction.

2 Data sets

The extensive Van Allen Probes, THEMIS, Cluster and GOES multi-instrument data sets provide numerous opportunities to observe the magnetospheric response to the changes in the solar wind and interplanetary magnetic field monitored by Wind. The five THEMIS spacecraft were launched in 2007 and carry identical instruments and operated in highly elliptical, near-equatorial, orbits that precess about the Earth with apogees of 12, 20, and 30 Re and orbital periods of 1, 2, and 4 days. With the outermost two spacecraft ARTEMIS now at the Moon, three THEMIS spacecraft remain on the innermost orbits. We use magnetic field data with 3 s time resolution from the THEMIS FGM triaxial fluxgate magnetometers (Auster et al., 2008). The ESA electrostatic analyzer on the THEMIS spacecraft measures the distribution functions of 0.005 to 25 keV ions and 0.005 to 30 keV electrons over 4Pi-str and provides accurate 3 s time resolution plasma moments, pitch angle and gyrophase particle distributions (McFadden et al., 2008).

The two Van Allen Probes were launched in August 2012 into nearly identical equatorial and low inclination (~10°) orbits with perigee altitudes of 605 and 625 km and apogee altitudes of 30410 and 30540 km (Mauk et al., 2012). Both satellites carry identical sets of instruments to measure charged particle populations, fields, and waves in the inner magnetosphere. In this paper, we employ observations from the Energetic Particle, Composition, and Thermal Plasma Suite (ECT: MagEIS, 20-4000 keV for electrons) (Spence et al., 2013; Blake et al., 2013). Electric and Magnetic Field Instrument Suite and Integrated Science (EMFISIS) (Kletzing et al., 2013), and the Electric Field and Waves Suite (EFW) (Wygant et al., 2013). In particular, we inspect electric and magnetic field observations with 11 and 4 s time resolution, respectively, and differential particle flux measurements with ~ 11 s (spin period) time resolution. The electric field data were obtained from sites http://www.space.umn.edu/rbspefw-data and CDAWEB where they are presented in an MGSE (modified GSE) coordinate system. They provide two components Y and Z of the electric field. Both components are in the spin plane of the spaceraft and are measured with the 50 m long booms. The spin axis X is oriented within 37 degrees of the Earth-Sun line. The spin axis component of the electric field can be obtained from the E dot B = 0 assumption. For this to succeed the magnetic field should be at least 15 degrees out of the spin plane. To calculate Van Allen Probes plasma flow velocities we converted the electric field data from modified MGSE coordinates into GSE coordinates. Additionally we used magnetic field data from GOES 13 and 15 with 0.5 s time resolution (Singer et al., 1966) and Cluster with 4 s time resolution (Balogh et al., 1997). We use Wind solar wind magnetic field and SWE plasma data with 3 s (Lepping et al., 1995) and 1 min, respectively (Ogilvie et al., 1995).

3 Observations

Figure 1 presents Wind magnetic and plasma data from 15:30 to 16:10 UT on February 27, 2014. The arrival of the shock at Wind at 15:50 UT (X, Y, Z GSM = (220.9, 93.9, 30.7 Re)) is revealed by an enhancement in the interplanetary magnetic field strength from 6 to 16 nT and total plasma velocity from 350 to 420 km/s. The IMF had positive Bx and negative By components during the whole interval that both increased the shock arrived. The solar wind density increased from 18 to 45 cm-3, and the dynamic pressure increased from 3 to 13 nPa. This fast forward (FF) shock was oblique. Its normal was calculated using magnetic field coplanarity and pointed in the GSM [nx, ny, nz] =[-0.8, -0.4, -0.3] direction, i.e., antisunward, dawnward, and southward. Consequently the shock should first strike the northern dusk bow shock and magnetopause. i.e., it has a spiral IMF orientation. We will use the direction of the shock normal to interpret the timing results for the IP shock arrival observed by THEMIS, GOES, Cluster and the Van Allen Probes spacecraft for this event.

Figure 2 shows the GSM locations of The THEMIS, Cluster, Van Allen Probes and GOES spacecraft at ~ 16:50 UT (Their coordinates are given in Table 1). All the spacecraft located in the solar wind observed the enhanced magnetic field strength, densities, velocities and temperatures associated with the IP shock. The shock induced disturbances were seen just upstream from the bow shock by Cluster 1 and 3, located at high southern postnoon latitudes at 16:48:46 UT and 16:48:57 UT, respectively .

Figures 3 (a, b) show the THEMIS D and A observations of the magnetic field, plasma and energy spectra of ion fluxes from 16:40 to 17:20 UT. The spacecraft were initially located in the magnetosheath. At 16:49:04 UT the IP shock hit THEMIS D as indicated by enhanced densities, magnetic field strength and velocities. Particles from low to high energies showed the increase of energy and enhanced fluxes. The shock produced compression caused the bow shock to move inward at 16:49:36 UT, past the spacecraft as indicated by the decrease in the magnetic field strength and, decrease in density and temperature and spectra expected for its entry into the solar wind. THEMIS A observed the IP shock at 16:49:12 UT and in about 1 min and 34 s later its magnetic field, density and temperature traces indicate that the bow shock moved inward past THEMIS A.

Figures 4 (a, b) show GOES 13 and 15 observations of the magnetic field from 16:40 to 17:20 UT. Following the arrival of the transmitted IP shock at GOES 13 near local noon at 16:50:07 UT there was a sharp increase of magnetic field variations with amplitudes of ~70 nT in the H component. The shock induced compression was so strong that at 17:02 UT GOES 13 briefly entered the sheath. The shock front was then detected at GOES 15 in the morning local hours 33 sec later at 16:50:40 UT, where it caused a gradual increase of the magnetic field amplitudes by ~ 20 nT followed by compressional pulsations that fall in the category of Pc5 pulsations.

The upper and middle panels of Fig. 5 (a, b) present the Van Allen Probes A and B magnetic field and electric observations from 16:40 to 17:20 UT. The arrival of the shock characterized by a strong (~ 50 nT) increase in the total magnetic field strength and bipolar variations in all three components of the electric field at ~ 16:50:26 UT at Probe B and 7 sec later at Probe A. The initial electric field perturbations in the Ey component observed by Van Allen Probes A and B were directed dawnward with amplitudes of -9.4 and - 8.2 mV/m, respectively, but ~ 4 minutes later the sense changed direction towards dusk (with amplitudes of 5.3 and 5.8 mV/m). We interpret these variations as due to a compression of the magnetosphere followed by a reflection (Samsonov et al., 2007). The Ez and Ex components show variations with amplitudes that are a factor of 1.5-2 smaller than those of the Ey component. The bipolar electric field waveforms are followed by geomagnetic pulsations with periods of ~ 330 s that damp within ~ 30 min.

Figures 6 (a, b) present Van Allen Probes A and B observations of the Ez component of the electric field and pitch angle distributions for electron energies of 31.5, 53.8, 108.3, 183.4, 231.8, and 342 KeV measured by the MagEIS instrument. The electrons exhibit enhanced intensities at all energies but the most intense occur at pitch angles near 90^o, immediately after the arrival of the IP shock. Kanekal et al. (2016) suggested that the shock-injection mechanism can be effective for energizing particles over a substantial range of pitch angles. The initial flux enhancement is more pronounced by comparison with the following pulses. One of the interesting feature in Figures 6 (a, b) is that the intensity of electrons in the energy range of 31.5-342 KeV exhibits a regular periodicity with periods corresponding to the ULF electric field waves. The oscillations in electron fluxes are in quadrature with the Ey component. This component is of special interest because some charged particles that drift azimuthally as a consequence of the gradient and curvature drifts in the Earth magnetic field can traverse this electric field acquiring a significant amount of energy. Figures 7 (a, b, c, d, e, f) present the response of the energetic electrons to the IP shock in the energy range from 31 to 183 keV. Panels d and b show that after the shock arrival the electron population increased, especially for the lower energies. In the electrical field of 15 mV/m electron fluxes increased by factors of 21 and 14 at Van Allen Probes B and A, respectively, in less than a drift period (panels e and f). The energetic electron fluxes do not display obvious phase differences across the energies. We interpret these observations as evidence for prompt energization of electrons due to shock induced ULF electric fields with an additional contribution for the initial acceleration from the compressional effect of the shock. It should be noted that electrons can be accelerated most significantly via drift resonance (Southwood and Kivelson, 1981) when resonant particles drift with the same velocity as the wave front. Claudepierre et al. (2013) showed Van Allen Probes observations of the energy dependence of the amplitude and phase of the electron flux modulations which were consequences of drift resonance between ~ 60 keV electrons and fundamental poloidal Pc5 waves. Hao et al. (2014) presented Van Allen Probes observations of electron injections caused by the IP shock and showed that the injected electrons with energies between 150 KeV and 230 KeV were in drift resonance with the excited poloidal ULF waves. Considering the process for energizing drift resonant electrons, the value for the E x B drift velocities of the particles in the wave fields provides important information. We calculated the Vx and Vy drift velocities at Van Allen Probes A and B for the interval from 16:40 to 17:20 UT and present them in the two bottom panels of Fig. 5 (a, b). The Vx and Vy components associated with the minimum peak of the Ey electric field are about -40 km/s and -15 km/s for Van Allen Probe B and -35 km/s and -6 km/s for Van Allen Probe A, i. e., the initial direction of the plasma flow is tailward and dawnward consistent with expectation for the spiral orientation of the IP shock.

Interaction with the initial fast mode pulse and subsequent ULF electrical field oscillations can have an important effect on particle acceleration. In considering the energization of electrons on February 27, 2014, an encounter with the observed electric field for a period of 240 s will transport the electrons earthward by δRe = 1.3 to 1.6 Re from their original position at L = 6.4 for Van Allen Probe A and at L = 7.1 for Van Allen Probe B. Conservation of the first adiabatic invariant implies that such particles will be energized by a factor of about 1.9 - 2.3 in only one cycle of the electric field pulsations. The studies of Wygant et al. (1994) using CRRES data and Foster et al. (2015) using Van Allen Probes data, and others have demonstrated that the tailward propagation of the strong shock-induced electric field impulse and subsequent ULF processes can result in the extremely fast acceleration of relativistic electron populations inside the plasmasphere.

Knowing the distances between the satellites and the lag times for the propagation of shock induced disturbances we calculated the shock propagation velocities. Table 1 summarizes the onset times of the shock driven encounters at different spacecraft. In the solar wind Cluster 1 observed the shock earlier than Cluster 3, respectively, that is the shock moved dawnward. The shock perturbations occurred almost simultaneously in the magnetosheath at Themis A and D (delta t < 10 s) suggesting the front strikes a broad region of the magnetopause at once. The shock induced impulse propagated antisunward, southward and both dawnward and, presumably, duskward (thick arrows in Fig. 2) from the point of origin on the magnetopause (depicted as a red oval in Fig. 2) that is consistent with the orientation of the IP shock. In the outer magnetosphere the propagation velocity for the disturbance was about 1348 km/s between Goes 13 and 15 but only about 390 km/s between Van Allen Probes B and A. We believe that the shock induced pulse propagated with the velocity of fast mode waves. The local fast mode speed can be evaluated from Van Allen Probe measurements of the magnetic field and density. At the time of the shock encounter Van Allen Probes A and B were in the high-density plasmasphere at L = 5.5 and L = 5.1, respectively. For a measured local magnetic field of 255 nT for Probe A and 220 nT for Probe B and density of ~ 200 cm-3 derived from the potential of both spacecraft, the fast-mode speeds will be ~ 395 km/s and 337 km/s, respectively, which are consistent with our estimates of the propagation velocity derived from the time difference of shock arrivals at the spacecraft. The decrease of the fast mode wave speed in the plasmasphere relative to that in the outer magnetosphere agrees well with earlier studies (e.g., Wilken, 1982; Foster et al., 2016).

4 Statistical study of shock-initiated signatures of the electric field

The list of IP shocks used in this study was obtained from Heliospheric Shock Database mantained and generated by the University of Helsinki [http://ipshocks.fi]. They identify shocks by visual inspection and an automated shock detection algorithm. To be included in the database a shock should satisfy the following upstream to downstream jump conditions: Bdown/Bup > 1.2, Ndown/Nup > 1.2, Tdown/ Tup > 1/1.2, for FF Vup-Vdown >20 km/s. The normal vector of the shock (n) was calculated from the magnetic field data and velocities using the mixed mode method (Abraham-Shrauner and Yun, 1976). When there is data gap in the velocity components the normal was calculated using magnetic field coplanarity (Colburn and Sonett, 1966).

In view of the importance of the electric field in energizing particles we performed a statistical study of Ey variations of the electric field and associated plasma drift Vx and Vy velocities during the passage of interplanetary shocks We identified more than 60 events observed by Van Allen Probes A and B associated with FF IP shocks for the period from 2013 to 2015. The shocks arrived from Wind with lag times in the time range from 26 min to 58 min and produced magnetic field perturbations in the magnetosphere from several to 130 nT. Discontinuities in the solar wind plasma such as shocks have often been considered as possible triggers for the release of energy stored within the magnetotail in the form of magnetospheric substorms. Most previous studies of shocks leading to substorms have relied on ground magnetometer observations. Recently it has been shown that the use of global auroral images to identify substorm onsets has some advantages over many other alternative substorm onset signatures, such as low-latitude Pi2 pulsations, auroral kilometric radiation (AKR), and dispersionless particle injections and magnetic field dipolarization at geosynchronous orbits (e.g., Liou et al., 2000). To identify substorms triggered by shocks in our study we considered negative magnetic bays by examining the westward auroral electrojet AL index at the times when SSC were determined from low-latitude ground magnetograms.. As a quantitative definition for the substorm bay does not exist we used the criteria of Liou et el. (2003) that there should be a sharp decrease in AL of at least 100 nT occurring within a 20 min window starting at the SSC. We found that shocks triggered a substorm in the magnetosphere in 17 of the 30 examined events. Further study whether these negative magnetic bays are unique identifiers of substorms is beyond the scope of the paper. Other effects in the magnetosphere initiated by IP shocks are perturbations in the electric field (Wygant et al., 1994) and the radiation belt (Blake et al., 2015). Understanding and predicting such responses is important for reducing the risks associated with space exploration. We found that 55 events showed an electron enhancement at energies of 32-54 keV measured by MagEIS at all local time and three of them were accompanied by intensity decreases at higher energies. Five events showed a decrease of the 32-54 keV energy electrons observed in the nightside magnetosphere.

The passage of a shock causes electric field perturbations and their amplitudes to increase in proportion to the intensity of the IP shocks. The E field vectors prior to each compression differ greatly from those during the compressional activity. We classified the shock-induced electric field signatures into four different groups according to the examples presented in the upper panels of Fig. 8. Group A presents a negative pulse in the Ey component, B group presents a negative-positive pulse, C group presents a positive pulse and D group presents pulsations. Figure 9 presents occurrence patterns for events with the four different signatures of the electric field initiated by IP shocks. It provides evidence that they are local time dependent. Negative and bipolar pulses predominate on the dayside with positive pulses occur on the nightside. The ULF electric field pulsations of Pc and Pi types produced by IP shocks are observed at all local times and in the range of periods from several tens of seconds to several minutes. We believe that the magnetic field as well the electric field pulsations initiated by IP shocks are generated by a wide variety of mechanisms including plasma instabilities, transient reconnection, pressure pulses, and often correspond to field line resonances. Their characteristic features are determined to large extent by local time. In the dayside magnetosphere typical pulsations are of the Pc5 type. Sometimes they last for more than twenty wave cycles without noticeable damping which could be explained by a continuous input of the solar wind energy into the magnetosphere. In the nightside magnetosphere during substorms, the generation of Pi2 pulsations is more common. They exhibit an irregular form, last 3-5 wave cycles, and often exhibit damping. Figure 10 presents periods of the pulsations (measured for the first wave cycle of oscillations) as a function of radius and shows that periods increase with increasing radius. A simple explanation for this behavior of pulsation frequencies with radial distance can be given in terms of standing Alfvén waves along resonant field lines (Sugiura and Wilson, 1964). The length of the field lines, the magnetic field strength, and the plasma density distribution determine the Alfvén velocity, and the periods of the pulsations. This plot indicates that most electric field pulsations of the Pc5 type in the dayside magnetosphere at $L < 6$ are produced by field line resonances.

Figure 11 presents the amplitudes and direction of the initial Ey response to IP shocks in the X-Y GSM plane. The perturbations are negative (dusk-to-dawn) in the dayside magnetosphere (followed by the positive or oscillatory perturbations) and dominately positive (dawn-to-dusk direction) in the nightside magnetosphere, particularly mostly near the Sun-Earth line within an L-shell range from 2.5 to 5. The typical observed amplitudes range from 0.2 to 6 mV/m but can reach 12 mV during strong magnetic storms. In the nightside magnetosphere the response of Ey is rather weak and its ampludues do not not exceed 3 mV/m. To demonstrate the impact of IP shocks Fig. 12 shows amplitudes of the initial electric field variations (blue and red crosses) as a function of dynamic pressue observed at Wind. The electric field perturbations increase with the solar wind pressure and that the changes are especially marked in the dayside magnetosphere (red points) as this region is more fully exposed to compression than the nightside sector that is shielded from the frontside compression.

To determine the Vx direction of the plasma after the impact of IP shocks we used the formula $V = E \times B/B^2$ for the 60 events under the study. Figure 13 presents the amplitudes and direction of the plasma drift velocities Vx that occur in response to IP shocks (in red - sunward and in blue – tailward directions). The direction of the Vx component of plasma flow is in agreement with the direction of the Ey component (except three peculiar events) and is antisunward at all local times except the nightside magnetosphere, where it is sunward near the Sun-Earth line. The tailward velocities are associated with tailward magnetic field line motion in the dayside magnetosphere. Numbers show that the magnitudes of the flow velocities Vx range from 0.2 to 40 km/s and are a factor of 5 to 10 times stronger near noon as they correspond to greater variations of the electric field in this region.

Our results are consistent with the results of global 3D MHD code simulation for the geosynchronous magnetic field response in the nightside magnetosphere to IP shocks by Wang et al. (2010) presented in Fig. 14. The figure shows contours of delta IBzI and velocity vectors in the equatorial plane (blue regions - Bz negative, red regions - Bz positive). Their model revealed that when a IP shock sweeps over the magnetosphere there are mainly two regions in the nightside magnetosphere, a positive response region in Bz caused by the compressive effect of the shock and a negative response region (blue) which is associated with the temporary enhancement of earthward convection. They believe that the displacement of the nightside magnetopause caused by the IP shock launches a flow in the magnetosphere near the magnetopause that has a significant y-component, and converges toward the X axis. In the vicinity of the Sun-Earth line at ~ -5, -6 Re the flow diverges, producing both an earthward flow (consistent with the sunward direction of plasma flow in the nightside magnetosphere presented in Fig. 13) and a tailward flows.

As the direction of the shock normal should determine the direction of propagation of transient perturbations and expected flow direction in the magnetosphere initiated by an IP shock we calculated plasma drift velocities Vy for 30 events for which the Ex component could be obtained from E dot B = 0. We categorized them into two groups for spiral and orthospiral orientation of the shock normal. Figure 15 presents the amplitudes and direction of the plasma drift velocities Vy observed by Van Allen Probes A and B in response to IP shocks (red- sunward Vx and blue – tailward Vx directions) for spiral and orthospiral orientations of IP shocks. We excluded several events from the list of shocks that lacked well defined shock normal. As anticipated, the shock orientation controls the sense of dawn/dusk flows in magnetosphere. The observed directions of velocity Vy predominately agree with those expected for the given shock normal orientation: dawnward for shocks that sweeps dawnward across the magnetosphere, duskward for shocks that sweep duskward.

5 Conclusions

We presented multipoint observations concerning the response of the electric and magnetic fields, plasma and particles in the magnetosphere to an IP shock on February 27, 2014. We used a multi-spacecraft timing method to determine the propagation speed and direction of the wave front induced by the IP shock. The propagation velocity of the disturbances was about 1348 km/s between Goes 13 and 15 in the outer magnetosphere, but it was only about 390 km/s between Van Allen Probes B and A in the inner magnetosphere consistent with expectations for a plasmasphere with limited radial extent. We deduced that the initial encounter of the IP shock with the magnetopause occurred on the post-noon magnetosphere and the shock induced impulse propagated as a fast mode wave both dawnward and, presumamly, duskward from the point of origin consistent with the spiral orientation of the IP shock. The multipoint measurements provide evidence for a dusk-dawn oscillatory electrical field in the dayside equatorial magnetosphere with a peak-to-peak amplitude of ~ 15 mV/m for a period of 30 min. Both spacecraft observed enhanced fluxes of energetic electrons in the range of energies from 31.5 - 342 KeV and their intensity shows a regular periodicity with periods corresponding to the electric field pulsations. We interpret these observations as evidence for prompt energization of electrons due to shock induced ULF electric fields with an additional contribution for the initial acceleration from the compressional effect of the shock. An encounter with the observed electric field for a period of 240 s will transport the electrons earthward by δRe = 1.3 to 1.6 Re from their original positions at L = 6.4 for Van Allen Probe A and at L = 7.1 at Van Allen B. Conservation of the first adiabatic invariant implies that such a particle will be energized by a factor of about 1.9 - 2.3 in only one cycle of the electric field pulsations. The initial plasma flow velocity in the magnetosphere was directed tailward and dawnward, consistent with expectation for the spiral orientation of the IP shock.

We identified more than 60 events observed by Van Allen Probes A and B associated with FF IP shocks for the period from 2013 to 2015. The shocks arrived from Wind with lag times in the time range from 26 min to 58 min and produced magnetic field perturbations in the magnetosphere from several to 130 nT. We found that shocks triggered a substorm in the magnetosphere in 17 of the 30 examined events. Taking advantage of the multipoint Van Allen Probes observations, we performed a statistical study of Ey variations of the electric field and associated plasma drift Vx and Vy flow velocities during the passage of interplanetary shocks. The Ey perturbations are negative (dusk-to-dawn) in the dayside magnetosphere (followed by positive or oscillatory perturbations) and dominately positive (dawn-to-dusk direction) in the nightside magnetosphere, particularly near the Sun-Earth line within an L-shell range from 2.5 to 5. The typical observed amplitudes range from 0.2 to 6 mV/m but can reach 12 mV during strong magnetic storms. We showed that electric field perturbations increase with solar wind pressure and that the changes are especially marked in the dayside magnetosphere. The direction of the Vx component of plasma flow is in agreement with the direction of the Ey component and is antisunward at all local times except the nightside magnetosphere, where it is sunward near the Sun-Earth line but antisunward towards dawn and dusk. The flow velocities Vx range from 0. 2 to 40 km/s and are a factor of 5 to 10 times stronger near noon as they correspond to greater variations of the electric field in this region**.** We investigated how the electric field perturbations deviate from the preceding undisturbed period and demonstrated that the shock-induced electric field signatures can be classified into four different groups according to the initial Ey electric field response. These signatures are local time dependent. Negative and bipolar pulses predominate on the dayside with positive pulses occur on the nightside. The ULF electric field pulsations of Pc and Pi types produced by IP shocks are observed at all local times and in the range of periods from several tens of seconds to several minutes. We believe that that most electric field pulsations of the Pc5 type in the dayside magnetosphere at $L < 6$ are produced by field line resonances. One of the most important results from the present study is that the direction of the shock normal determines the direction of the propagation of the shock induced magnetic and plasma disturbances. The observed directions of velocity Vy predominately agree with those expected for the given spiral or orthospiral shock normal orientation. Our results are consistent with the results of global MHD code simulation of the geosynchronous nightside magnetic field response to IP shock by Wang et al. (2010).

Table 1. Times of encounter of the IP shock with the spacecraft and their locations in GSM coordinates

S/C	Time	Position GSM [X, Y, Z] Re		
Wind	15:50:12	220.90	93.92	31.49
Cluster 1	16:48:46	13.10	7.82	-9.44
Cluster 3	16:48:57	12.60	7.73	-10.16
THEMIS D	16:49:04	11.03	0.48	1.10
THEMIS A	16:49:12	9.22	4.39	0.53
Probe A	16:50:33	4.86	-1.69	0.12
Probe B	16:50:26	5.33	-1.39	-0.10
GOES 13	16:50:07	6.51	-0.60	0.99
GOES 15	16:50:40	2.71	-6.02	0.45

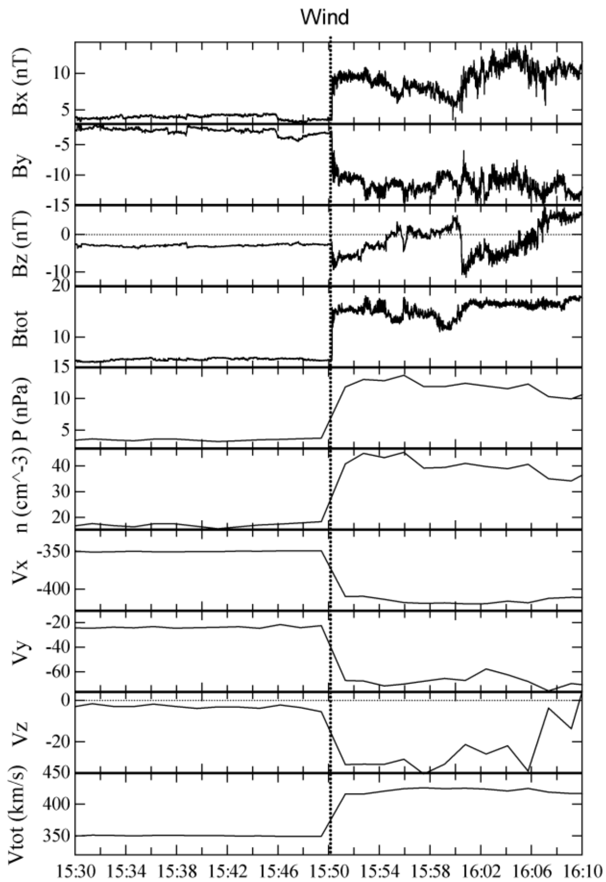

Figure 1. Wind observations of magnetic field and plasma in GSM coordinates from 15:30 UT to 16:10 UT on February 27, 2014. Dashed line shows the time of arrival of an interplanetary shock.

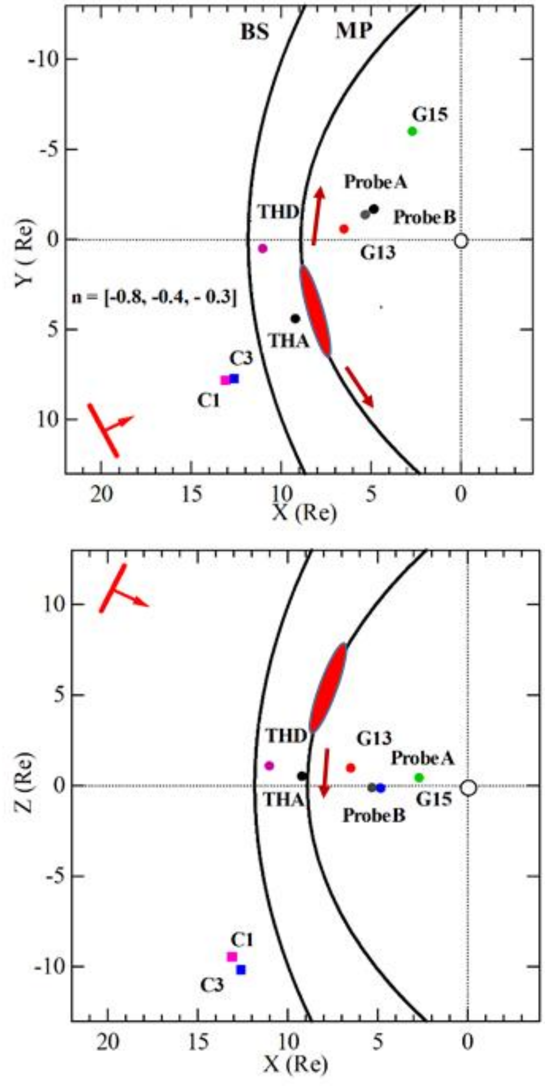

Figure 2. GSM locations of Cluster 1 and 3, THEMIS A, D, Van Allen Probes A and B and GOES 13 and 15 in the X-Y and Z-Y GSM planes at ~ 1650 UT on February 27, 2014. The meaning of the solid oval and thick arrows will be discussed in the text later.

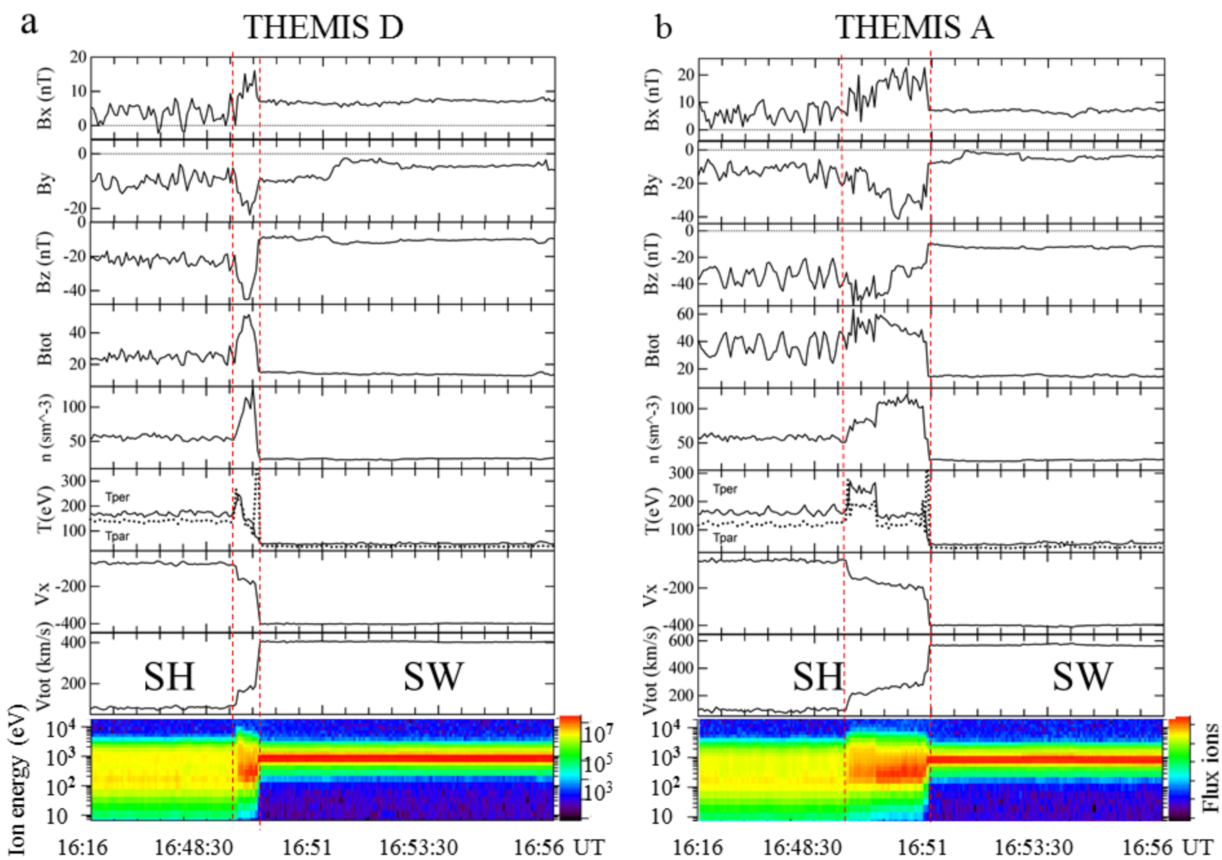

Figures 3 (a, b). THEMIS A (a) and THEMIS D (b) observations of magnetic field in GSM coordinates plasma and energy spectra of ion fluxes from 16:16 UT to 16:56 UT on February 27, 2014. At 16:49:01 UT the IP shock hit THEMIS D as indicated by enhanced densities, magnetic field strength and velocities. Particles from low to high energies showed the increase of energy and enhanced fluxes. The shock produced compression caused the bow shock to move inward at 16:49:36 UT, past the spacecraft as indicated by the decrease in the magnetic field strength and, decrease in density and temperature and spectra expected for its entry into the solar wind. THEMIS A observed the IP shock at 16:49:12 UT and in about 1 min and 34 s later its magnetic field, density and temperature traces indicate that the bow shock moved inward past THEMIS A.

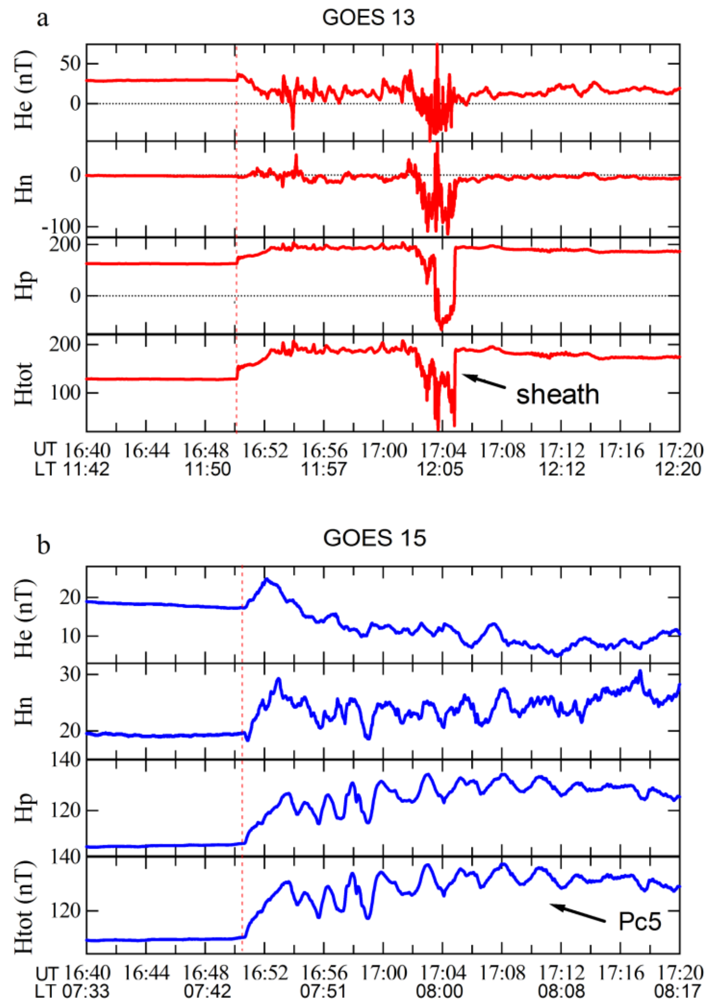

Figures 4 (a, b). GOES 13 (a) and GOES 15 (b) magnetic fields observations in PEN coordinate from 16:40 UT to 17:20 UT on February 27, 2014. Hp is perpendicular to the satellite's orbital plane, He pointing earthward parallel to the satellite-Earth center line, and Hn is perpendicular to both Hp and He and pointing eastward.

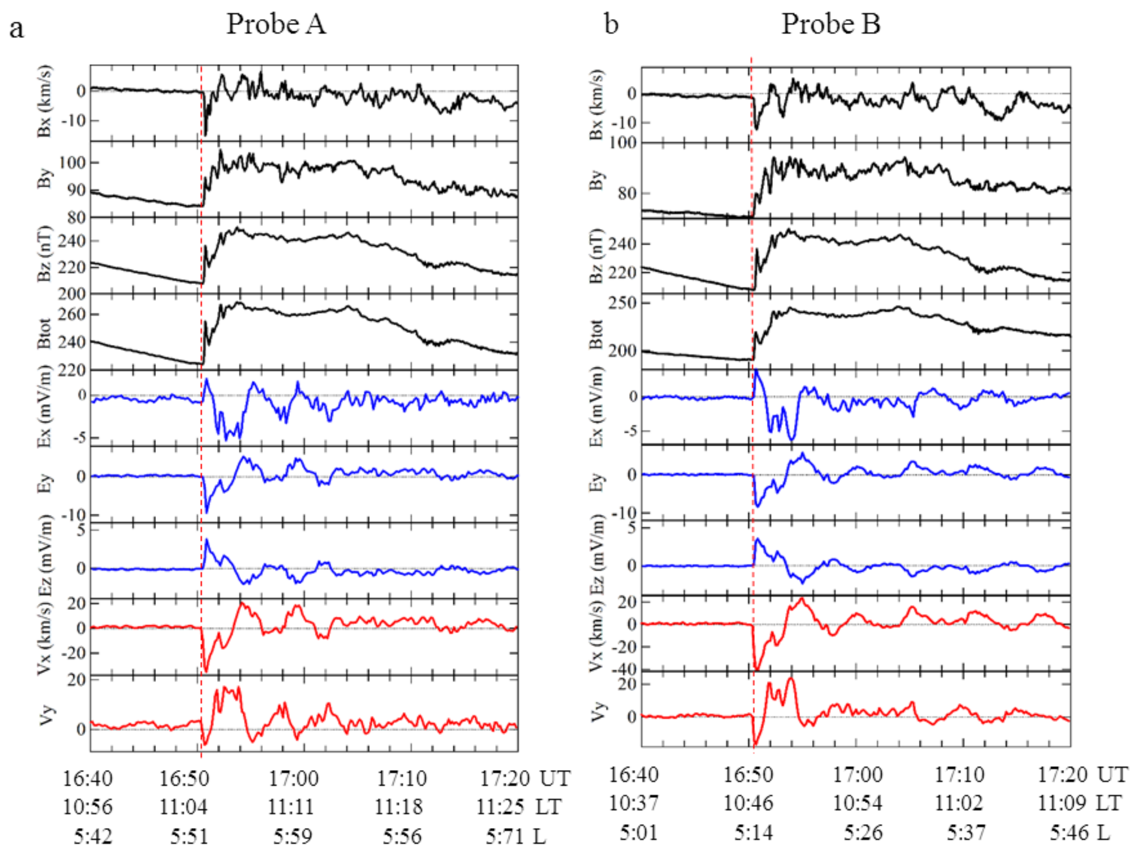

Figures 5 (a, b). Van Allen Probes A (a) and B (b) magnetic and spin-fit electric field observations and the Vx and Vy plasma flow velocities in GSE coordinates from 16:40 UT to 17:20 UT on February 27, 2014.

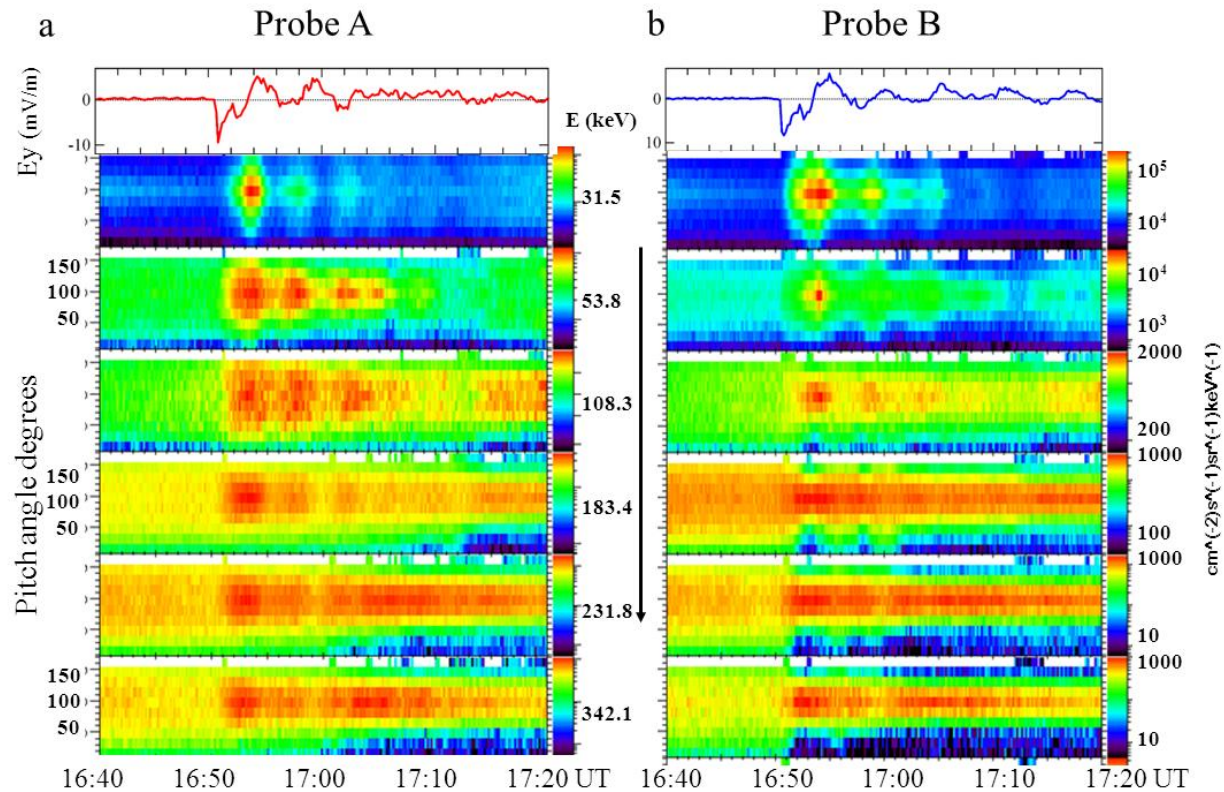

Figures 6 (a, b). Van Allen Probes A (a) and B (b) Ey component of the electric field and pitch angle distributions of electron fluxes in the range of energies from 31.5 to 342 KeV, measured by MagEIS instrument from 16:40 UT to 17:20 UT on February 27, 2014. The log fluxes are color coded according to the color bar shown in the right panel.

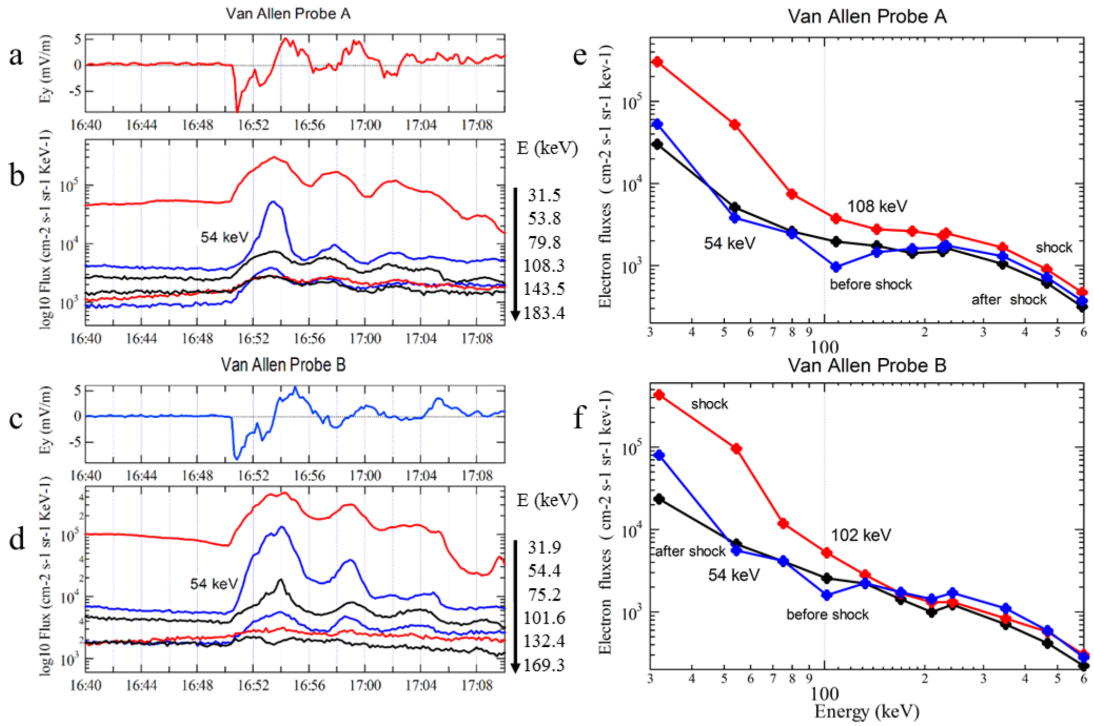

Figures 7. Response of the energetic particles to the transmitted IP shock. Panels a and c show measurements of the Ey component of the electric field. Panels b and d show electron fluxes for the energies ranging from 31.5 to 180 keV at Van Allen Probes A and B. Panels e and f show energetic electron spectra observed at Probe A and B before the shock (at 16:48 UT), after the first peak (at 16:53 UT) and 18 min after the shock (at 17:08 UT).

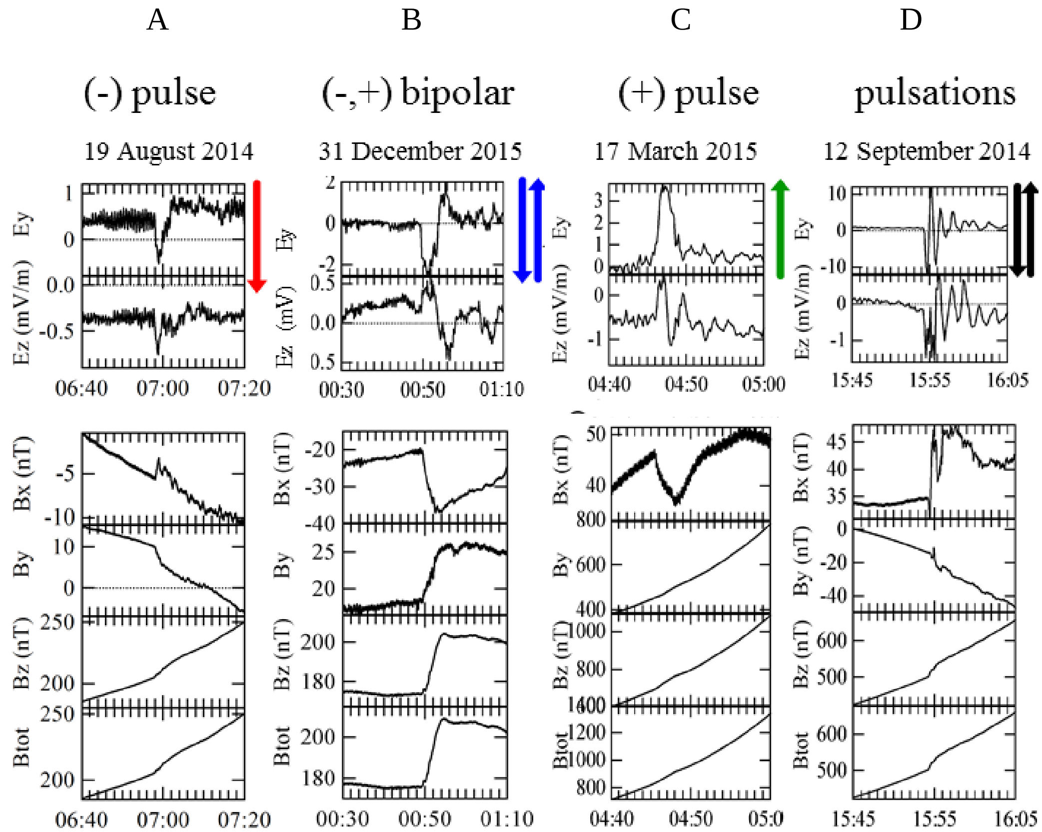

Figure 8. Examples of observed Ey initial variation, including a negative pulse (A), a negative-positive waveform (B), a positive pulse and pulsations (upper panels) and the corresponding magnetic field response (bottom panels).

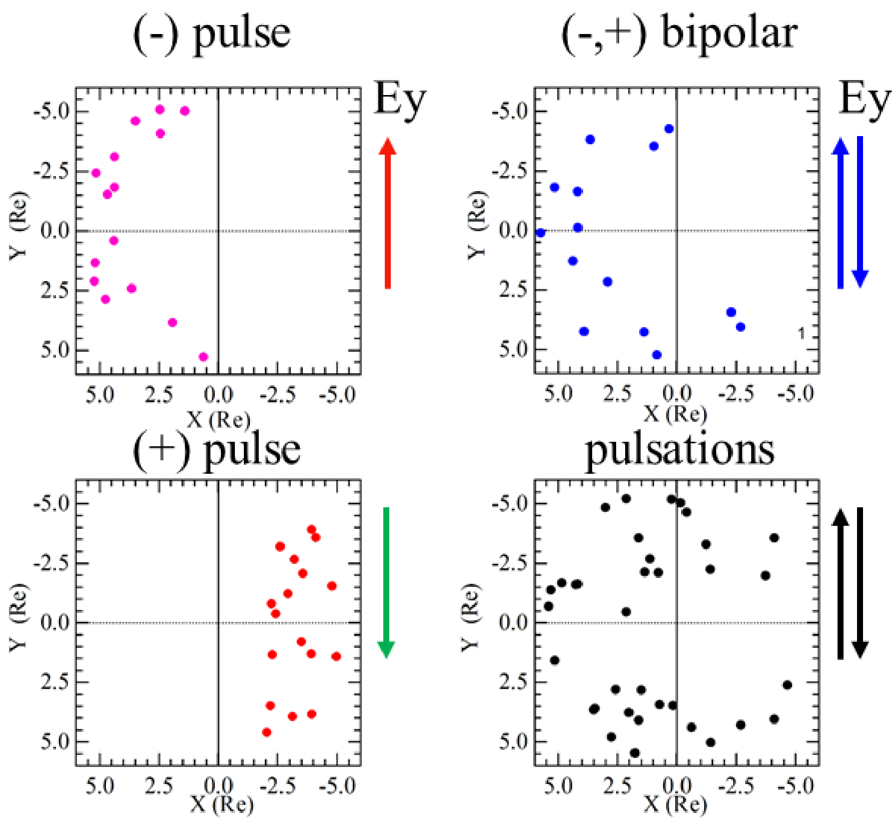

Figure 9. GSM locations where event in each of the four groups were observed in the X-Y plane.

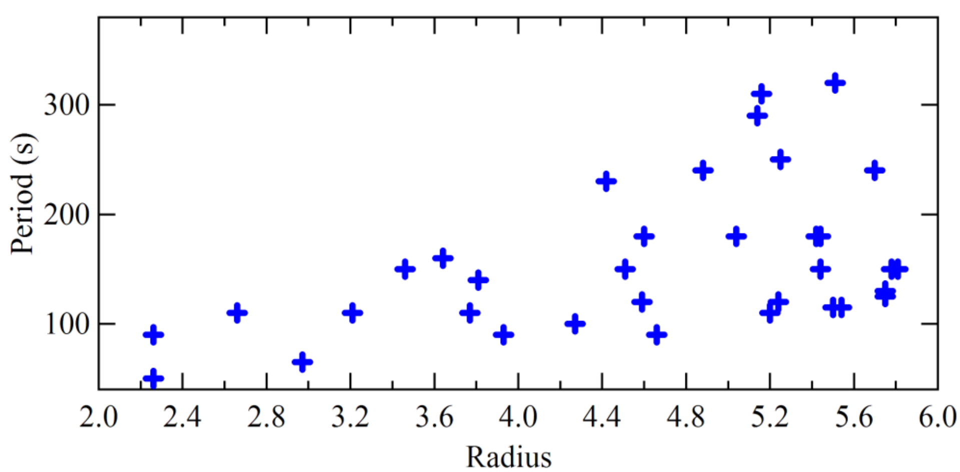

Figure 10. Periods of pulsations, initiated by IP shocks as a function of radius.

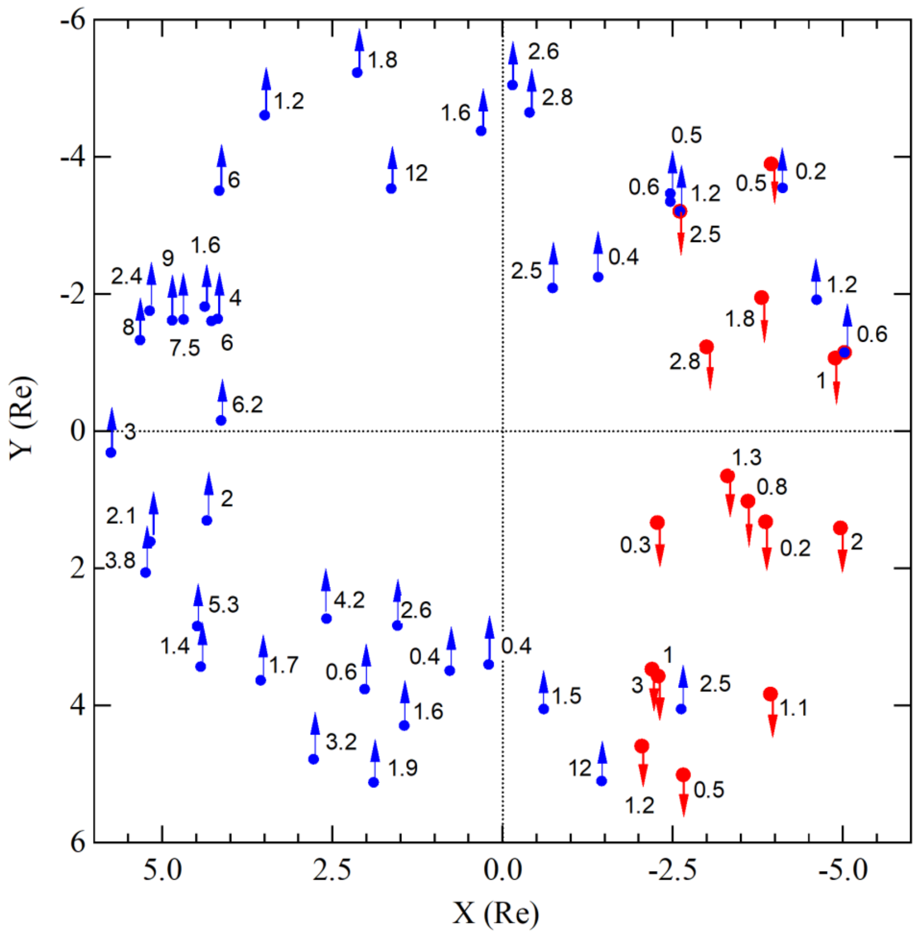

Figure 11. Amplitudes and direction of initial Ey response to IP shocks in the X-Y GSM plane (red dawn-duskward and blue duskward-dawn direction).

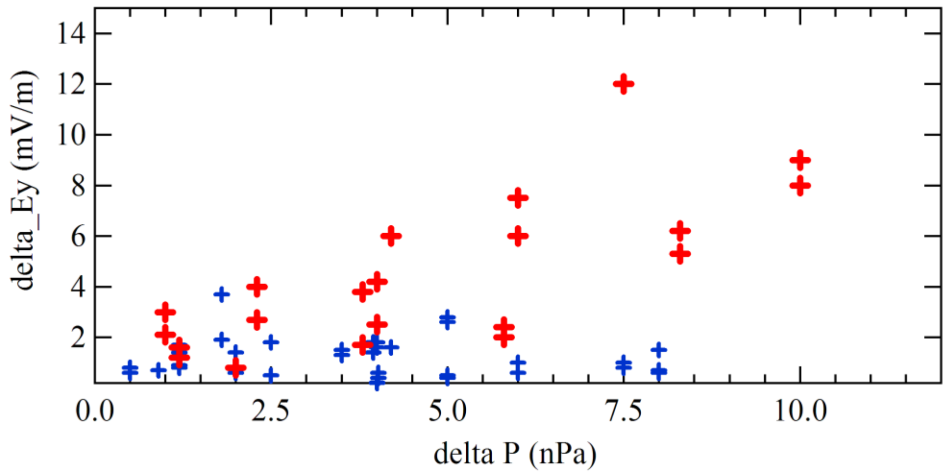

Figure 12. Amplitudes of initial Ey variations (blue and red points) caused by a shock as a function of intensity variations of dynamic pressure observed at Wind for 60 events.

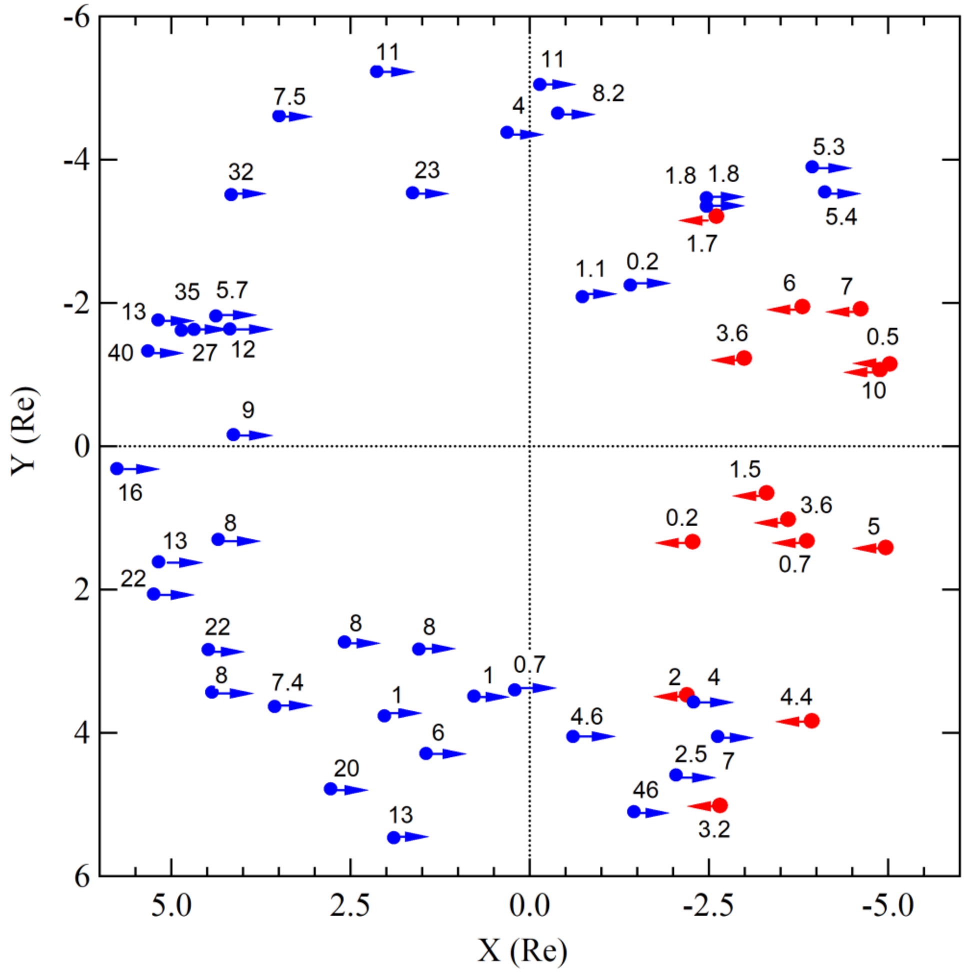

Figure 13. Amplitudes and direction of the plasma drift velocities $V_x=E \times B/B^2$ observed by Van Allen Probes A and B in response to interplanetary shocks (red - sunward and blue – tailward direction).

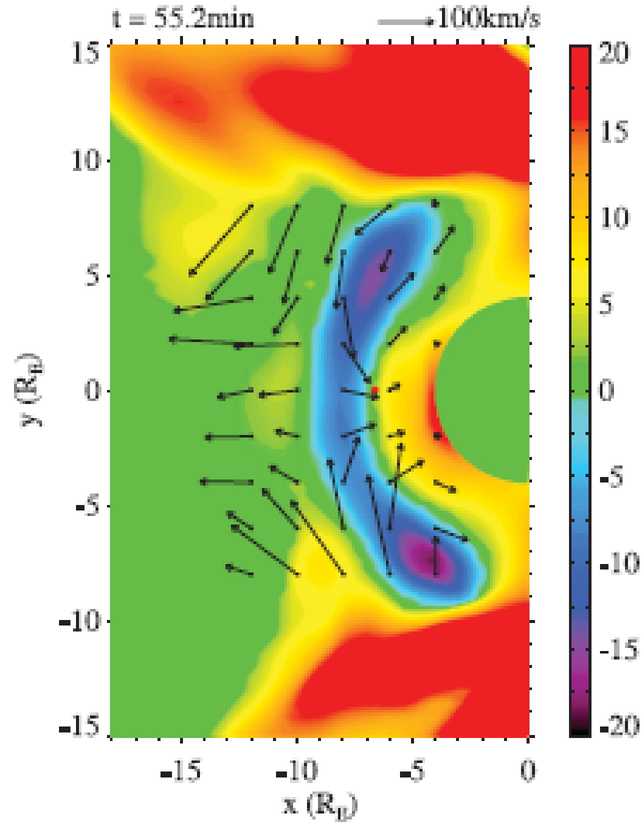

Figure 14. Results of nightside geosynchronous magnetic field response from the global MHD code simulation of IP shock (Wang et al., 2010). The arrows represent velocity vectors on the equatorial plane.

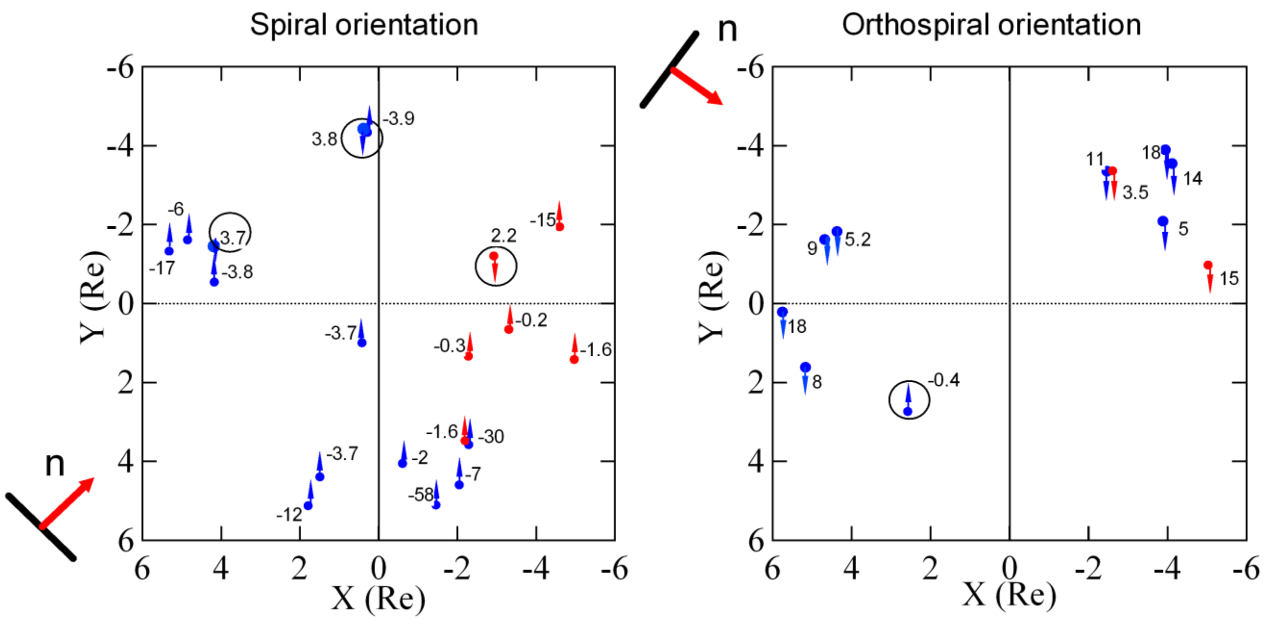

Figure 15. Amplitudes and direction of Vy plasma drift velocities observed by Van Allen Probes A and B in response to interplanetary shocks for spiral and orthospiral orientations (red - sunward and blue – tailward Vx directions).

6 Data availability.

Data used in the paper are available publicly at http://cdaweb.gsfc.nasa.gov/istp_public/ (Coordinated Data Analysis Web). GOES data can be found at http://satdat.ngdc.noaa.gov/sem/goes/data/new_full/. The electric field data were obtained from sites http://www.space.umn.edu/rbspefw-data. The list of IP shocks used in this study was obtained from site :http://ipshocks.fi.

Team list:

Galina Korotova, David Sibeck, Scott Thaller, John Wygant, Harlan Spence, Craig Kletzing, Vassilis Angelopoulos, and Robert Redmon

Author contributions:

G. Korotova drafted and wrote the paper and all others commented it.
G. Korotova, D.Sibeck, S. Thaller and R. Redmon were the primary contributors to this work.
S. Thaller- programming, software development, consulting regarding use of Van Allen electric field data.
J. Wygant -consulting regarding use of Van Allen electric field data.
H. Spence -consulting regarding use of Van Allen plsma data
C. Kletzing -consulting regarding use of Van Allen Magnetometer data
V. Angelopoulos -consulting regarding use of THEMIS data

The authors declare that they have no conflict of interest.

Acknowledgements. The Van Allen Probes mission is supported by NASA. NASA GSFC's CDAWEB provided Wind and GOES observations, while SSCWEB provided Van Allen Probes EPHEMERIS. The work by GIK at the University of Maryland was supported by grants from NASA NNX15AW86G S01 and NSF AGS-1207445. The work by the EFW team at the University of Minnesota was supported by APL contract to UMN 922613 under NASA contract to APL NAS5-01072.

References

Abraham-Shrauner, B., and Yun, S. H.: Interplanetary shocks seen by Ames Plasma Probe on Pioneer 6 and 7, J. Geophys. Res., 81, 2097-2102, DOI: 10.1029/JA081i013p02097, 1976.

Araki, T.: A physical model of the geomagnetic sudden commencement, AGU Geophys. Monogr., 81, 183–200, 1994.

Auster, H. U., Glassmeier, K.-H., Magnes, W., Aydogar, O., W. Baumjohann, W., Constantinescu, D., Fischer, D., Fornacon, K. H., Georgescu, E., Harvey, P., Hillenmaier, O., Kroth, R., Ludlam, M., Narita, Y., Nakamura, R., Okrafka, K., Plaschke, F., Richter, I., Schwarzl, H., Stoll, B., Valavanoglou, A., Wiedemann,M.: The THEMIS Fluxgate Magnetometer, Space Sci. Rev., 141, 235– 264, doi:10.1007/s11214-008-9365-9, 2008.

Blake, J. B, Carranza, P. A, Claudepierre, S. G., Clemmons, J. H., Crain, Jr. W. R., Dotan, Y., Fennell, J. F., Fuentes, F. H., Galvan, R. M., George, J. S., Henderson, M. G., Lalic, M., Lin, A. Y., Looper, M. D., Mabry, D. J., Mazur, J. E., McCarthy, B., Nguyen, C. Q., O'Brien, T.P., Perez, M. A., Redding, M. T., Roeder, J. L., Salvaggio, D. J., Sorensen, G. A., Spence, H. E., Yi, S., Zakrzewski M. P.: The Magnetic Electron Ion Spectrometer (MagEIS) Instruments Aboard the Radiation Belt Storm Probes (RBSP) Spacecraft**,** Space Sci. Rev.,179, 383-421, DOI**:** 10.1007/s11214-013-9991-8, 2013.

Bonnell, J. W., Mozer F. S., Delory, G.T., Hull, A.J., Ergun, R.E., Cully, C.M., Angelopoulos, V., and Harvey, P.R.: The electric field instrument (EFI) for THEMIS, Space Sci. Rev., 141, 303–341, DOI:10.100, 2008.

Claudepierre, S. G., Mann, I. R., Takahashi, K., Fennell, J. F., Hudson, M. K., Blake, J. B., Roeder, J. L., Clemmons, J. H., Spence, H. E., Reeves, G. D., Baker, D. N., Funsten, H.O., Friedel, R. H. W., Henderson, M. G., Kletzing, C. A., Kurth, W. S., MacDowall, R. J., Smith, C. W., and Wygant, J. R.: Van Allen Probes Observation of Localized Drift-Resonance Between Poloidal Mode Ultra-low Frequency Waves and 60 keV Electrons, Geophys. Res. Lett., 40, 4491-4497, DOI:10.1002/grl.50901, 2013.

Colburn, D. C., and Sonett, C. P.: Discontinuities in the solar wind, Space Science Reviews, 5(4):439–506, 1966.

Foster, J., Wygant, J., Hudson, M., Boyd, A., Baker, D., Erickson, P., Spence, H. E.: Shock-induced prompt relativistic electron acceleration in the inner magnetosphere. J. Geophys. Res. 120(3), 1661–1674, DOI:10.1002/2014JA020642, 2015.

Glassmeier, K. H., Heppner, C.: Travelling magnetospheric twin-vortices: Another case study, global characteristics and a model. J. Geophys. Res. 97, 3977-3992. DOI: 10.1029/91JA02464, 1992.

Guo, X. C., Hu, Y. Q., and Wang, C.: Earth's magnetosphere impinged by interplanetary shocks of different orientations, Chin. Phys. Lett., 22, 3221–3224, 2005.

Halford, A. J., McGregor, S. L., Murphy, K. R., Millan, R. M., Hudson, M. K., Woodger, C.A., Cattel, L. A., Breneman, A. W., Mann, I. R., Kurth, W. S., Hospodarsky, G. B., Gkioulidou, M., Fennell, J. F.: BARREL observations of an ICME-Shock impact with the magnetosphere and the resultant radiation belt electron loss. J. Geophys. Res. Space Phys.,J. Geophys. Res., 120, 2557–2570, DOI:10.1002/2014JA020873, 2015.

Hao, Y., Zong, Q.-G., Wang, Y., Zhou, X.-Z., Zhang, H., Fu, S., Pu, Z. Y., Spence, H. E., Blake, J. B., Bonnell, J., Wygant, J., and Kletzing, C.: Interactions of energetic electrons with ULF waves triggered by interplanetary shock: Van Allen Probes observations in the magnetotail, J. Geophys. Res., DOI: 10.1002/2014JA020023, 2014.

Kanekal, S. G., Baker, D. N., Fennell, J. F., Jones, A., Schiller, Q., Richardson, I. G., Li, X., Turner, D. L., Califf, S., Claudepierre, S. G., Wilson III, L. B., Jaynes, A.,. Blake, J. B., Reeves, G., Spence, H. E., Kletzing, C. A., and Wygant, J. R.: Prompt Acceleration of Magnetospheric Electrons to Ultra-Relativistic Energies by the 17 March 2015 Interplanetary Shock, J. Geophys. Res., DOI:10.1002/2016JA022596, 2016.

Kim, K.-H., Park, K. S., Ogino, T., Lee, D.-H., Sung, S.-K., and Kwak Y.-S.: Global MHD simulation of the geomagnetic sudden commencement on 21 October 1999, J. Geophys. Res., 114, A08212, doi:10.1029/2009JA014109, 2009.

Kletzing, C. A., Kurth, W. S., Acuna, M., MacDowall, R. J, Torbert, R. B., Averkamp, T., Bodet, D., Bounds, S. R., Chutter, M., Connerney, J., Crawford, D., Dolan, J. S., Dvorsky R., Hospodarsky, G. B., Howard, J., Jordanova, V., Johnson, R. A., Kirchner, D. L., Mokrzycki, B., Needell, G., Odom, J., Mark, D., Pfaff Jr., Phillips, J. R. , Piker, C.W., Remington, S. L., Rowland, D., Santolik, O., Schnurr, R., Sheppard, D., Smith, C. W., Thorne, R. M., and Tyler, J. J.: The Electric and Magnetic Field Instrument Suite and Integrated Science (EMFISIS) on RBSP, Space Sci. Rev., 179, 127–181, DOI:10.1007/s11214-013-9993-6, 2013.

Knott, K., Fairfield, D., Korth, A., and Young, D. T.: Observations near the magnetopause at the onset of the July 29, 1977, sudden storm commencement, J. Geophys. Res., 87, A8, 5888–5894, DOI: 10.1029/JA087iA08p05888, 1982.

Li, X., Roth, I., Temerin, M., Wygant, J. R., Hudson, M. K., Blake, J. B.: Simulation of the prompt energization and transport of radiation belt particles during the March 24, 1991 ssc. Geophys. Res. Lett. 20, 2423–2426, DOI: 10.1029/93GL02701, 1993.

Liou, K., Newell, P. T., Meng, C.-I. , Wu, C.-C., and Lepping, R. P.: Investigation of external triggering of substorms with Polar ultraviolet imager observations, J. Geophys. Res., 108, A10, 1364-1378, DOI:10.1029/2003JA009984, 2003.

Mitchell, D.G., Lanzerotti, L.J., Kim, C.K., Stokes, M., Ho, G., Cooper, S., Ukhorskiy, A., Manweiler, J.W., Jaskulek, S., Haggerty, D.K., Brandt, P., Sitnov, M., Keika, K., Hayes, J.R., Brown, L.E., Gurnee, R.S., Hutcheson, J.C., Nelson, K.S., Paschalidis, N., Rossano, E., Kerem, S.: Radiation Belt Storm Probes Ion Composition Experiment (RBSPICE), Space Sci. Rev., 179, 263-308, DOI:10.1007/s11214-013-9965-x, 2013.

Mauk, B. H., Fox, N. J., Kanekal, S. G., Kessel, R. L., Sibeck, D. G., and Ukhorskiy A.: Science objectives and rationale for the radiation belt storm probes mission, Space Sci. Rev., 179, 3–27, DOI:10.1007/s11214-012-9908-y, 2012.

McFadden, J. P., Carlson, C. W., Larson, D., Ludlam, M., Abiad, R., Elliott, B., Turin, P., Marckwordt, M., and Angelopoulos, V.: The THEMIS ESA plasma instrument and in-flight calibration, Space Sci. Rev., 141, 277, DOI:10.1007/s11214-008-9440-2, 2008.

Nopper, Jr. R. W., Hughes, W. J., MacLennan, C. G., and McPherron, R. L.: Impulse-excited pulsations during the July 29, 1977, event, J. Geophys. Res., 87 (A8), 5911-5916, DOI: 10.1029/JA087iA08p05911, 1982.

Ogilvie, K. W., Chornay, D. J., Fritzenreiter, R. J., Hunsaker, F., Keller, J., Lobell, J., Miller, G., Scudder, J. D., Sittler Jr., E.C., Torbert, R. B., Bodet, D., Needell, G., Lazarus, A. J., Steinberg, J. T., Tappan, J. H., Mavretic, A., Gergin, E.: A comprehensive plasma instrument for the WIND spacecraft, Space Sci. Rev., 71, 55–77, DOI:10.1007/ BF00751326, 1995.

Oliveira, D. M., and Raeder, J.: Impact angle control of interplanetary shock geoeffectiveness: A statistical study, J. Geophys. Res., 120, 6, 4313–4323, DOI: 10.1002/2015JA021147, 2015.

Samsonov, A. A., Sibeck, D. G., and Imber, J.: MHD simulation for the interaction of an interplanetary shock with the Earth's magnetosphere, J. Geophys. Res., 112, A12220, DOI: 10.1029/2007JA012627, 2007.

Schiller, O., Kanekal, S. G., Jian, L. K., Li, X., Jones, A., Baker, D. N., Jaynes, A., and Spence, H. E.: Prompt injections of highly relativistic electrons induced by interplanetary shocks: A statistical study of Van Allen Probes observations, Research Letter, 10.1002/2016GL071628, 2016.

Schmidt, R., Pedersen, A.: Signatures of storm sudden commencements in the electric field measured at geostationary orbit (GEOS-2), Phys. Scr., 37, 3, 491–495, 1988.

Shinbori, A., Ono, T., Iizima, M., Kumamoto, A.,and Oya, H.: Sudden commencements related plasma waves observed by the Akebono satellite in the polar region and inside the plasmasphere region, J. Geophys. Res., 108, A12, 1457, DOI:10.1029/2003JA009964, 2003.

Shinbori, A., Ono, T., Iizima, M., and Kumamoto, A.: SC related electric and magnetic field phenomena observed by the Akebono satellite inside the plasmasphere, Earth, Planets Space, 56, 269–282, 2004.

Sibeck, D. G.: A model for the transient magnetospheric response to sudden solar wind dynamic pressure variations. J. Geophys. Res. 95, A4, 3755–3771, DOI:10.1029/JA095iA04p03755, 1990.

Singer, H. J., Matheson, L., Grubb, R., Newman, A., and. Bouwer, S. D.: Monitoring space weather with the GOES magnetometers, Proc. SPIE Int. Soc. Opt. Eng., 2812, 299–308, 1996.

Southwood, D. J., and Kivelson, M. G.: Charged particle behavior in low-frequency geomagnetic pulsations: 1. Transverse waves, J. Geophys. Res., 86, 5643–5655, DOI: 10.1029/JA086iA07p05643, 1981.

Southwood, D. J., and Kivelson, M. G.: The Magnetohydrodynamic Response of the Magnetospheric Cavity to Changes in Solar Wind Pressure, J. Geophys. Res. 95, 2301–2309, DOI: 10.1029/JA095iA03p02301, 1990.

Spence, H. E., Reeves, G. D., Baker, D. N., Blake, J. B., Bolton, M., Bourdarie, S., Chan, A. H. S., Claudepierre, G., Clemmons, J. H., Cravens, J. P., Elkington, S. R., Fennell, J. F., Friedel, R. H. W., Funsten, H. O., Goldstein, J., Green, J. C., Guthrie, A., Henderson, M. G , Horne, R. B., Hudson, M. K., Jahn, J.-M., Jordanova, V. K., Kanekal, S. G., Klatt, B. W., Larsen, B. A., Li, X., MacDonald, E. A., Mann, I. R., Niehof, J., O'Brien, T. P., Onsager, T. G., Salvaggio, D., Skoug, R. M., Smith, S. S., Suther, L. L., Thomsen, M. F., and Thorne, R. M.: Science Goals and Overview of the Energetic Particle, Composition, and Thermal Plasma (ECT) Suite on NASA's Radiation Belt Storm Probes (RBSP) Mission, Space Sci. Rev., DOI: 10.1007/s11214-013-0007-5 2013.

Takahashi, N., Kasaba, Y., Nishimura, Y., Shinbori, A., Kikuchi, T., Hori, T., Ebihara, Y., and Nishitani, N.: Propagation and evolution of electric fields associated with solar wind pressure pulses based on spacecraft and ground-based observations, DOI:10.1002/2017JA023990, 2017.

Tamao, T.: The structure of three-dimensional hydromagnetic waves in a uniform cold plasma, J. Geomagn. Geoelectr., 48, 89–114, doi: 10.5636/jgg.16.89, 1964.

Wang, C., Sun, T. R., Guo, X. C., and Richardson, J. D.: Case study of nightside magnetospheric magnetic field response to interplanetary shocks, J. Geophys. Res., 115, A10247, DOI:10.1029/2010JA015451, 2010.

Wilken, W., Goertz, C. K., Baker, D. N., Higbie, P. R. , Fritz , T. A.: The SSC on July 29, 1977 and its propagation within the magnetosphere. J. Geophys. Res. 87, 5901–5910, DOI: 10.1029/JA087iA08p05901, 1982.

Wilken, W., Baker, D. N., Higbie, P. R., Fritz, T.A., Olson, W. P., Pfitzer, K. A.: Magnetospheric configuration and energetic particle effects associated with a SSC: A case study of the

CDAW event on March 22, 1979, J. Geophys. Res. 91, 1459–1473, DOI: 10.1029/JA091iA02p01459, 1986.

Wygant, J., Mozer, F., Temerin, M., Blake, J., Maynard, N., Singer, H., and Smiddy M.: Large amplitude electric field and magnetic field signatures in the inner magnetosphere during injection of 15 MeV electron drift echoes, Geophys. Res. Lett., 21, 1739–1742, DOI: 10.1029/94GL00375., 1994.

Wygant, J. R., Bonnell, J. W., Goetz, K., Ergun, R. E., Mozer, F. S., Bale, S. D., Ludlam, M., Turin, P., Harvey, P. R., Hochmann, R., Harps, K., Dalton, G., McCauley, J., Rachelson, W., Gordon, D., Donakowski, B., Shultz, C., Smith, C., Diaz-Aguado, M., Fischer, J., Heavner, S., Berg, P., Malaspina, D. M., Bolton, M. K., Hudson, M., Strangeway, R. J., Baker, D. N., Li, X., Albert, J., Foster, J. C., Chaston, C. C., Mann, I., Donovan, E., Cully, C. M., Cattell, C. A., Krasnoselskikh, V., Kersten, K., Breneman, A., and Tao, J. B.: The electric field and waves instruments on the radiation belt storm probes mission, Space Sci. Rev., 179, 183–220, DOI:10.1007/s11214-013-0013-7, 2013.

Zong, Q.-G., Zhou, X.-Z., Wang, Y. F., Li, X., Song, P., Baker, D. N., Fritz, T. A., Daly, P. W., Dunlop, M., and Pedersen, A.: Energetic electron response to ULF waved induced by interplanetary shocks in the outer radiation belt, J. Geophys. Res., 114, A10204, DOI:10.1029/2009JA014393, 2009.